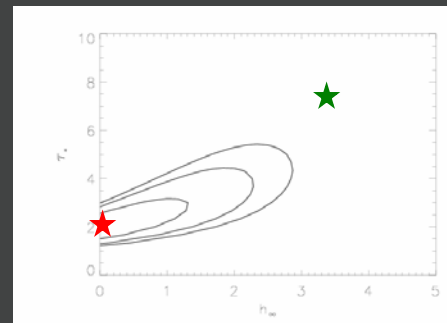
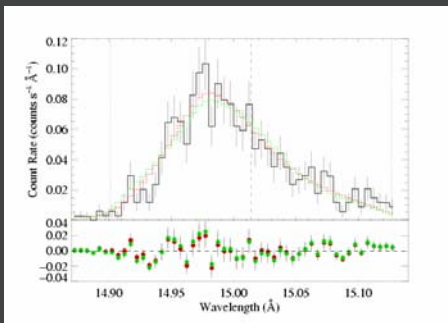
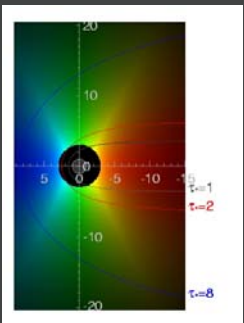


Quantitative Analysis of the Resolved X-ray Emission Line Profiles of O Stars

David Cohen
Department of Physics & Astronomy
Swarthmore College

with Maurice Leutenegger (Columbia University)



OUTLINE

1. The wind profile model and quantitative model fitting
2. Smooth wind models: constraints on mass-loss rates
3. Models with porosity: the τ_* - h_∞ trade-off
4. A note on grayness and opacity
5. What porosity lengths are realistic?

The basic smooth wind model:

$$L_\lambda = 8\pi^2 \int_{-1}^1 \int_{R_*}^{\infty} j e^{-\tau} r^2 dr d\mu$$

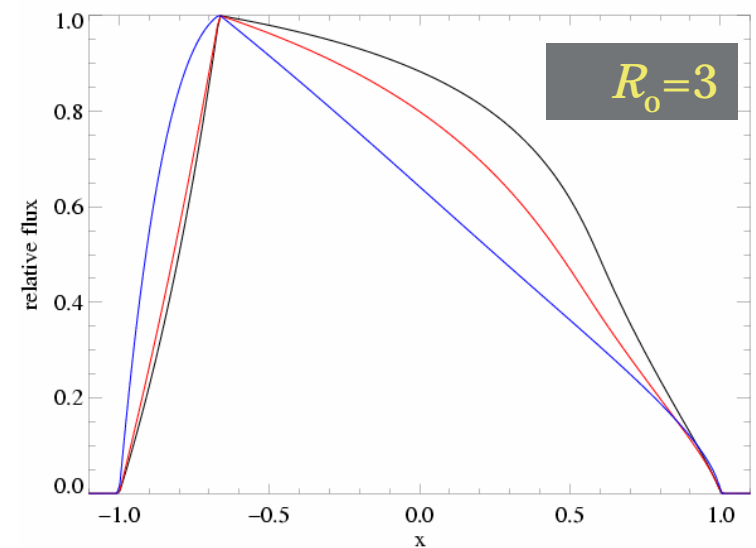
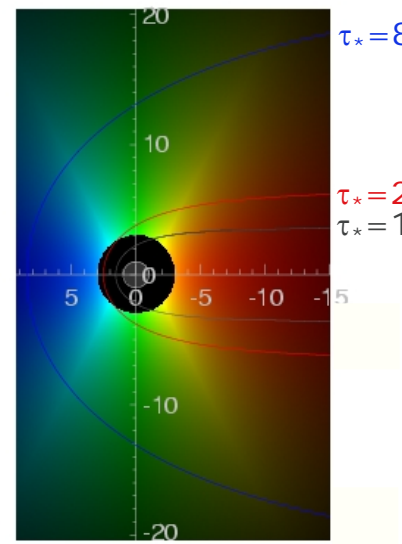
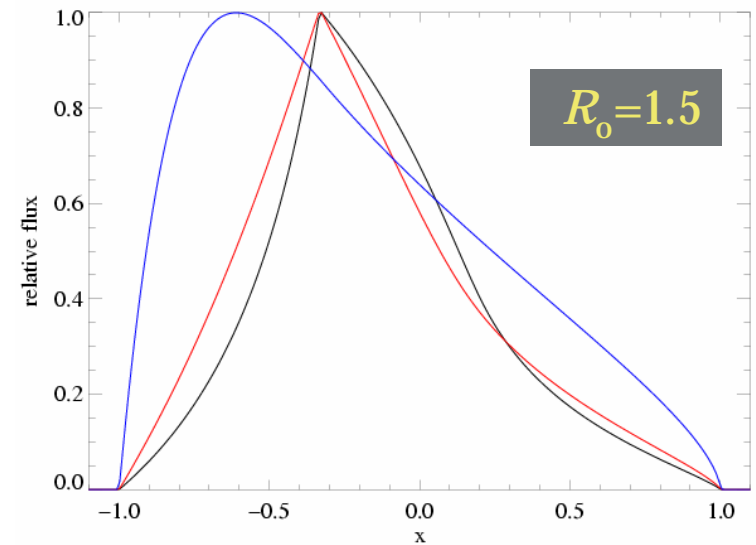
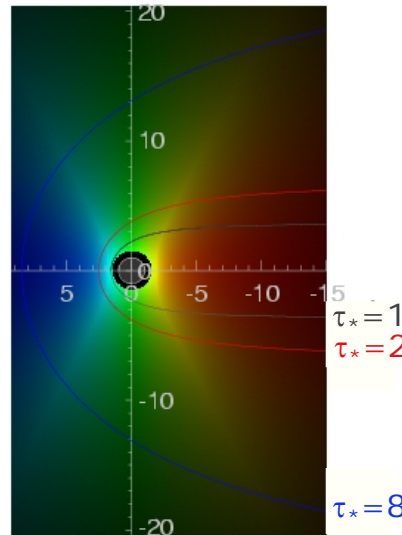
key parameters: R_o & τ_*

$$j \propto \rho^2 \text{ for } r/R_* > R_o, \\ = 0 \text{ otherwise}$$

$$\tau = \tau_* \int_z^{\infty} \frac{R_* dz'}{r'^2 (1 - R_*/r')^\beta}$$

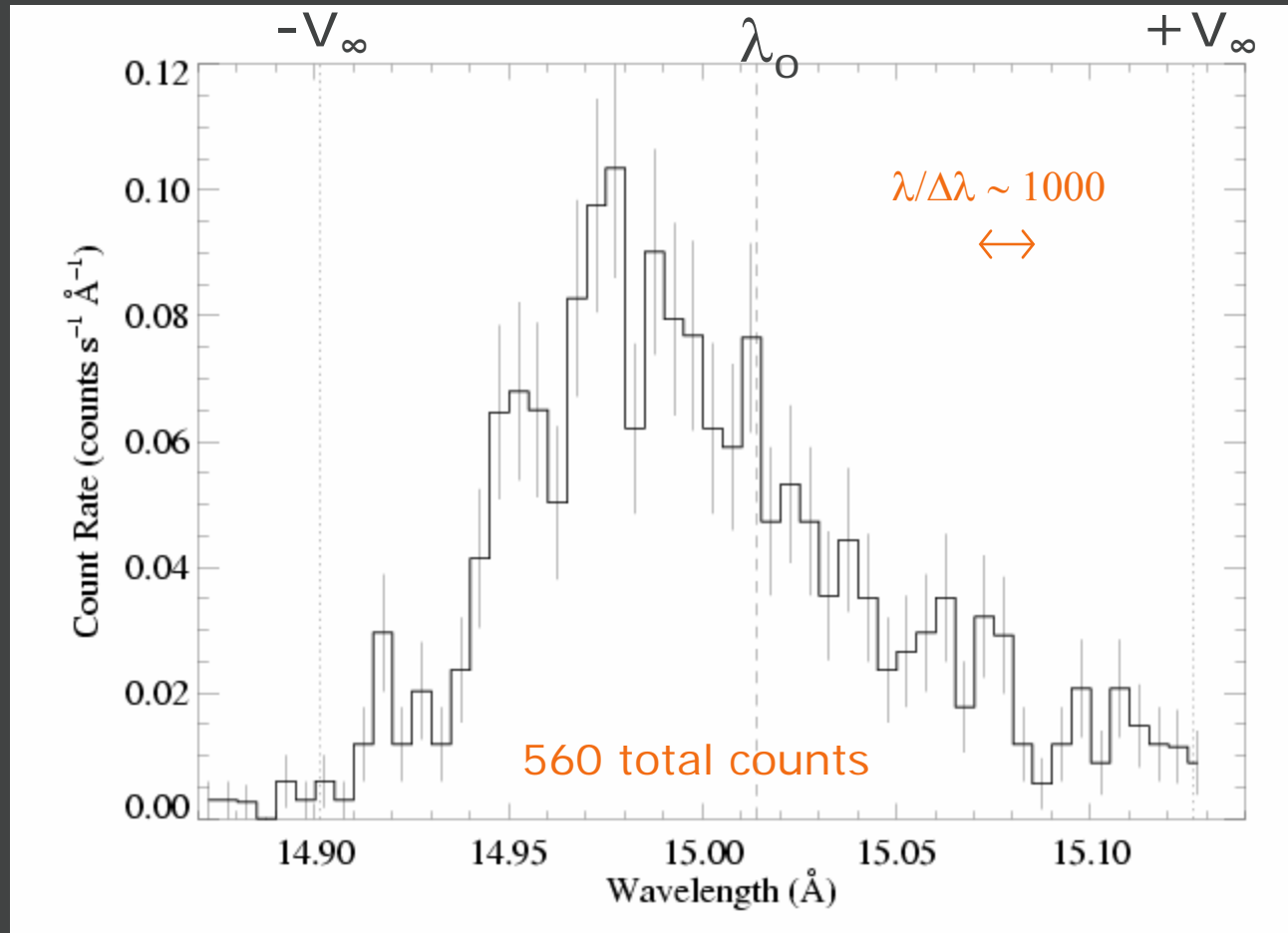
$$\tau_* \equiv \frac{\kappa M}{4\pi R_* v_\infty}$$

$\tau_* = 1, 2, 8$



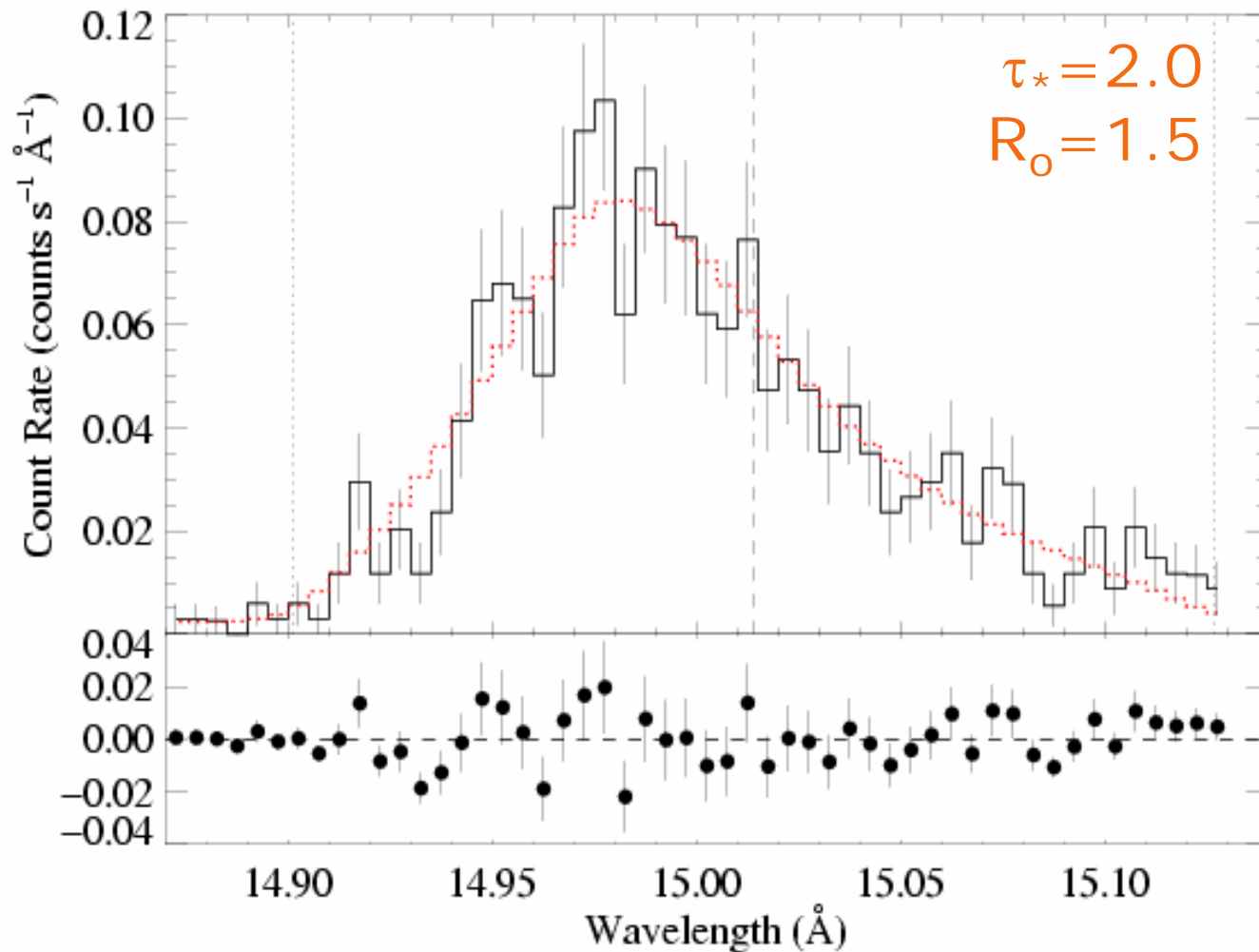
Highest S/N line in the ζ Pup *Chandra* spectrum

Fe XVII @ 15.014 Å



Fe⁺¹⁶ – neon-like; dominant stage of iron at $T \sim 3 \times 10^6$ K in this coronal (collisions up; spontaneous emission down) plasma

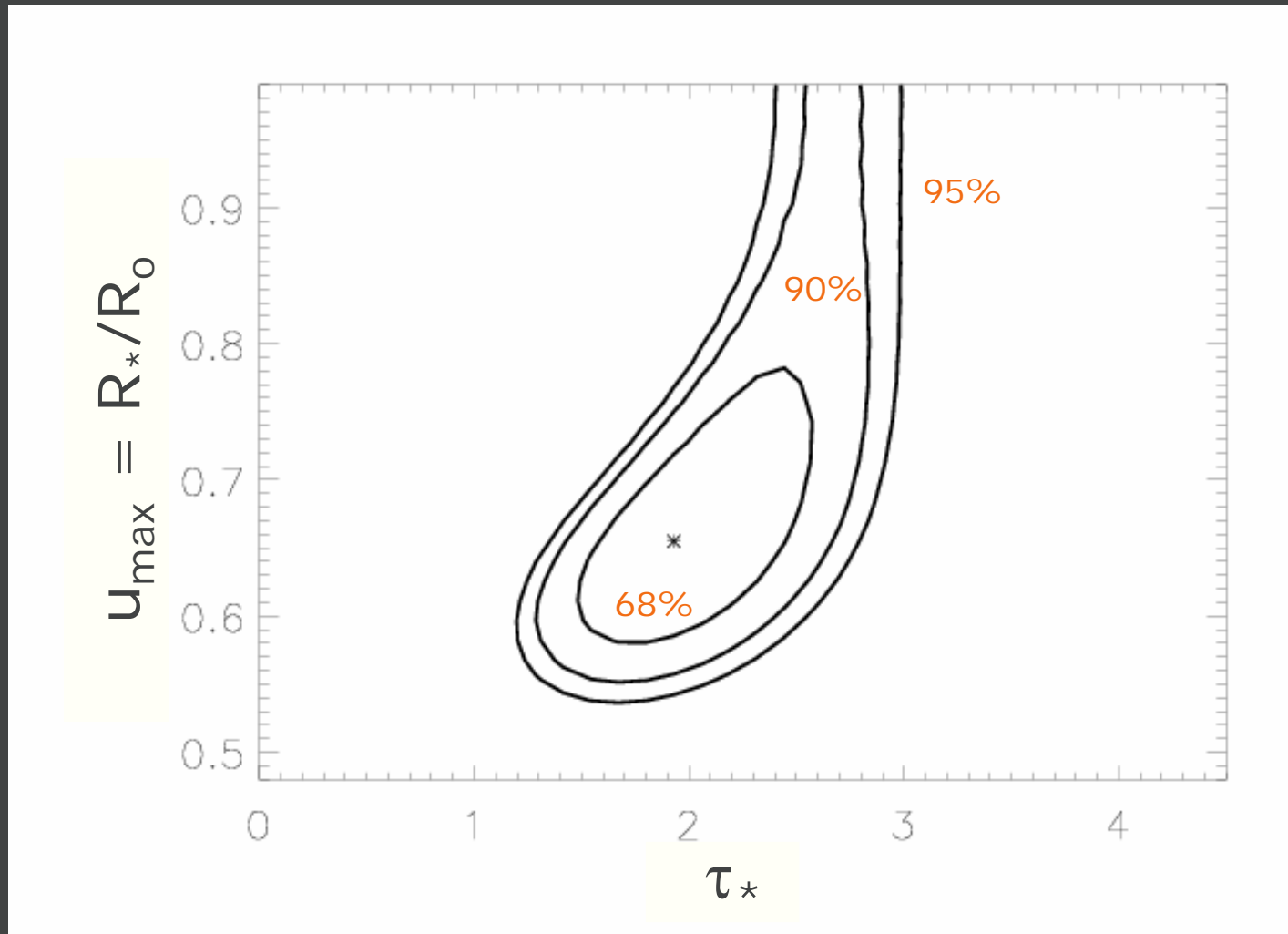
Best fit smooth wind model



Fit statistic: "Cash C" - maximum likelihood estimator for Poisson distributed data

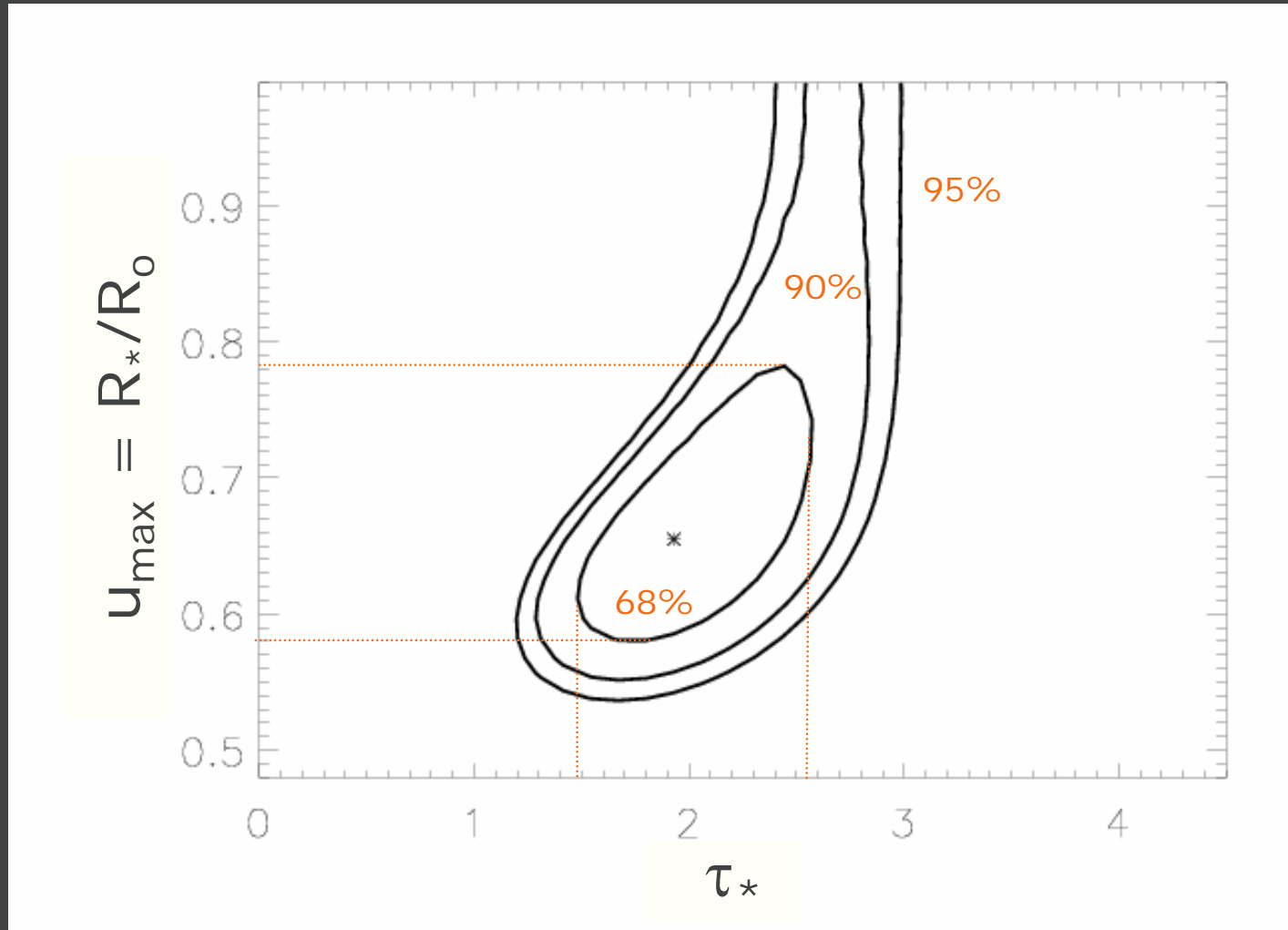
$C = 98.5$ for 103 degrees of freedom: $P = 19\%$

Confidence limits can be placed on the fitted model parameters



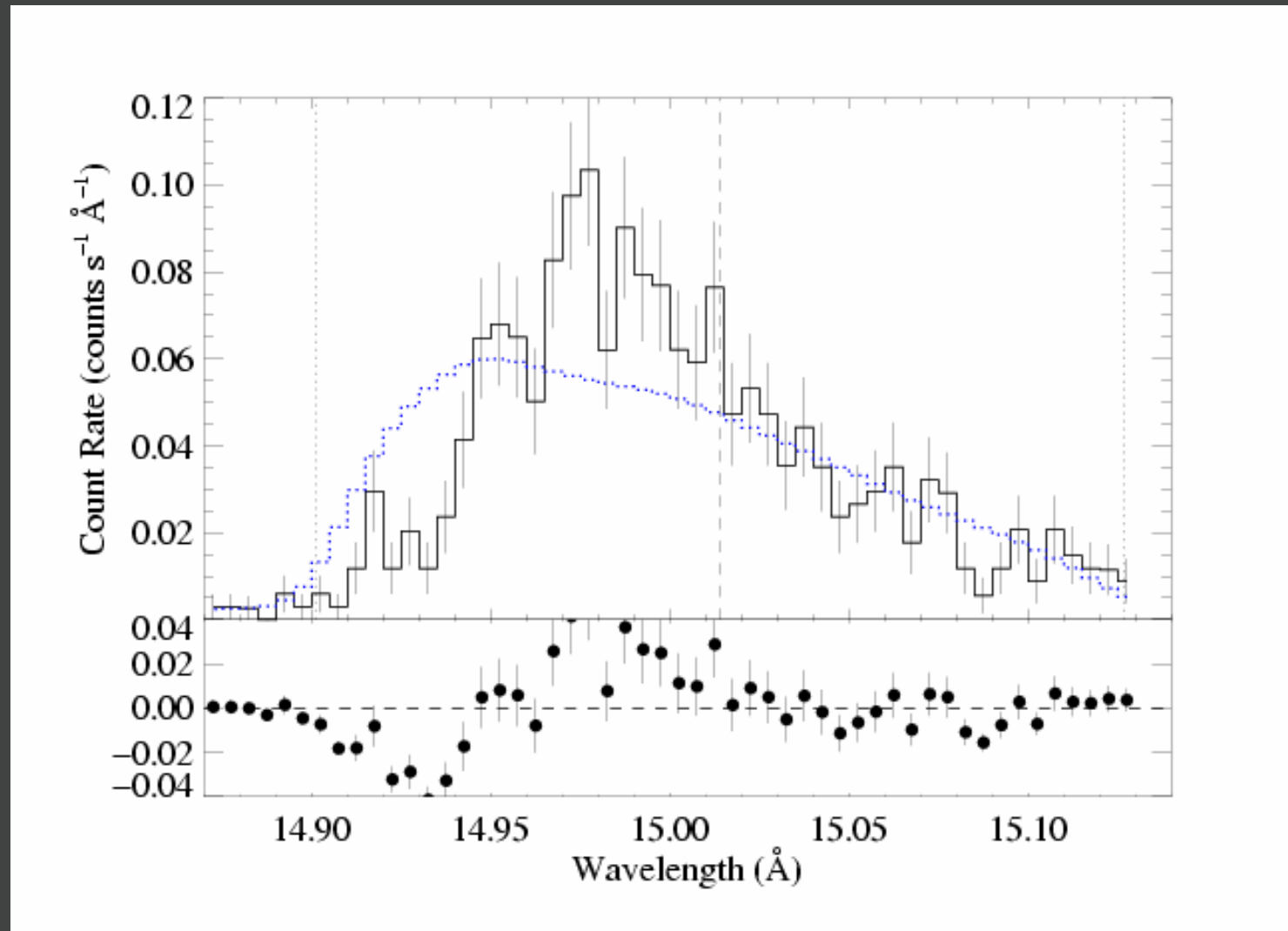
The confidence contours enclose regions where $\Delta C = C - C_{\min}$ exceeds a particular value ($\Delta C = 2.30$ corresponds to 68% for two parameters)

Confidence limits can be placed on the fitted model parameters

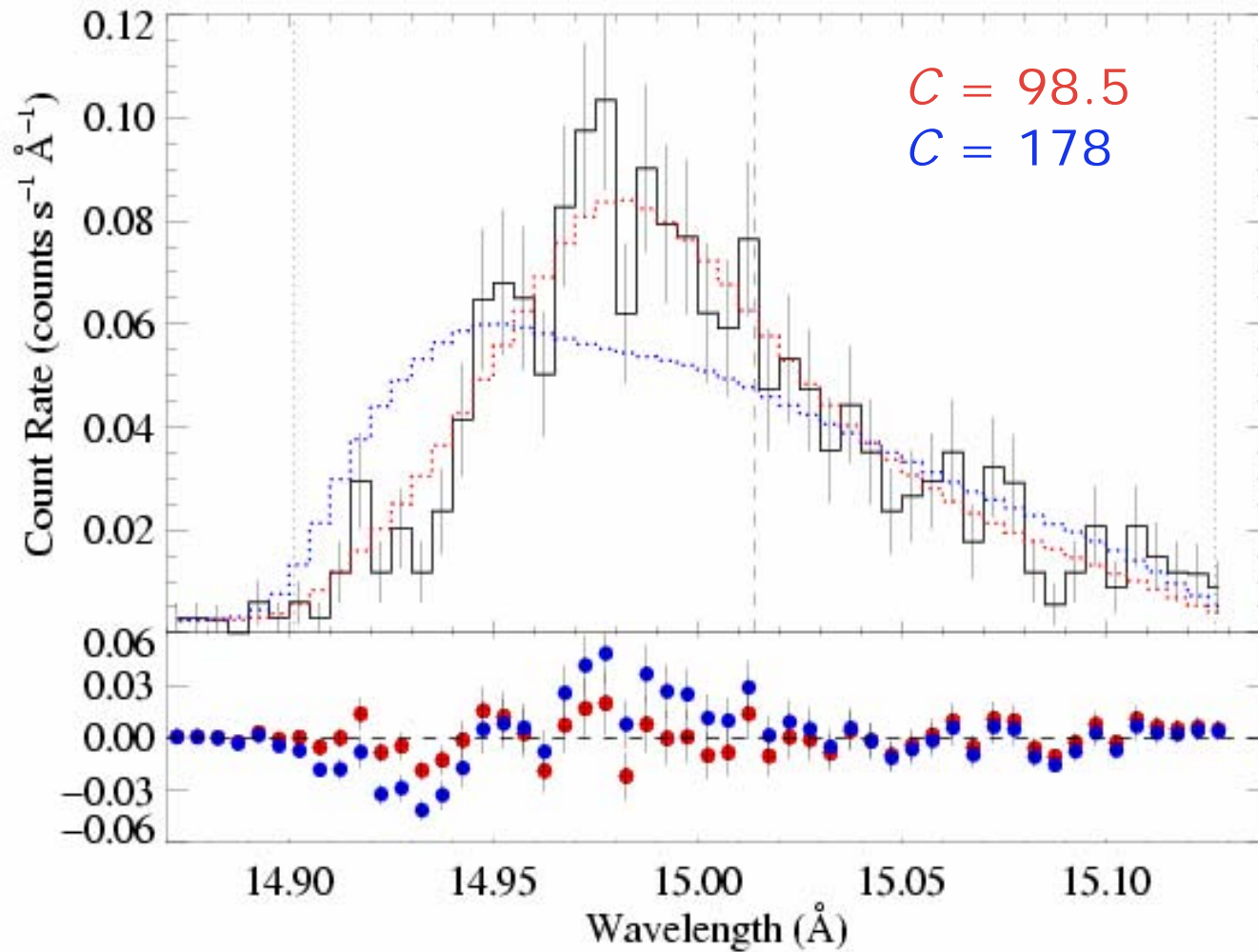


$1.5 < \tau_* < 2.6$ and $1.3 < R_0 < 1.7$

Best-fit smooth-wind model with $\tau_* = 8$



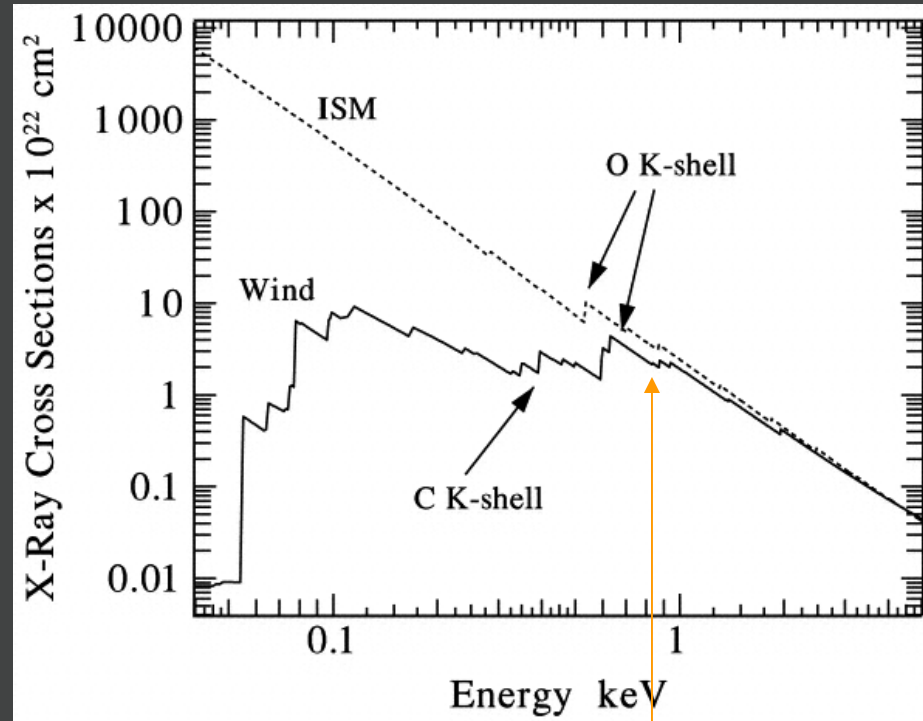
This is the value of τ_* expected from
 $\dot{M} \sim 7 \times 10^{-6} M_{\text{sun}}/\text{yr}$



Best-fit model – $\tau_* = 2$ – preferred over the $\tau_* = 8$ model with $>99.999\%$ confidence

$$\tau_* \equiv \frac{\kappa \dot{M}}{4\pi R_* v_\infty}$$

$$\dot{M}_{-6} = \frac{\tau_* R_{12} v_{2000}}{3.6 \kappa_{150}}$$

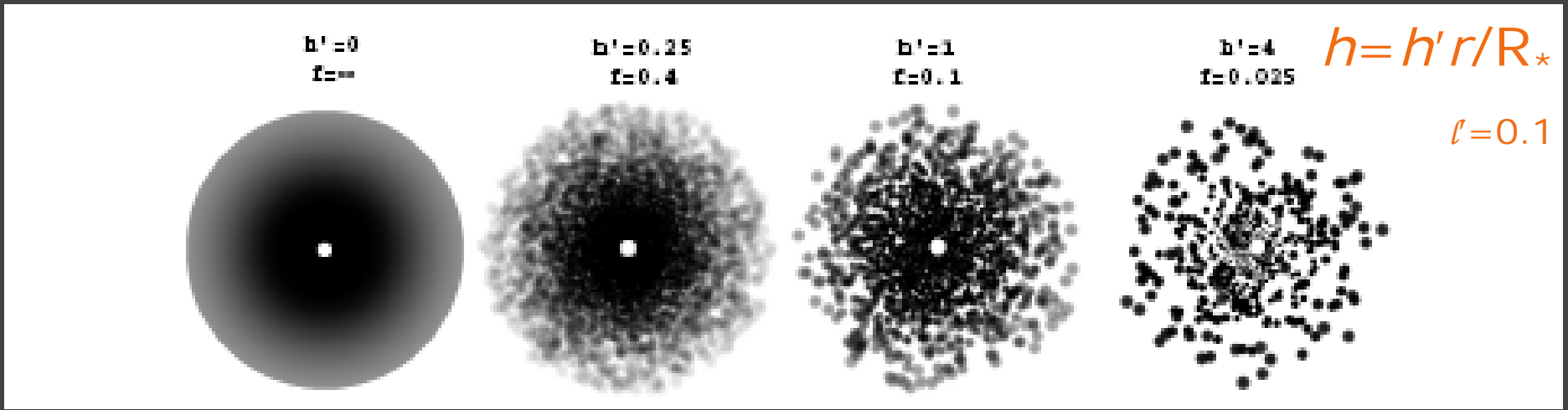


$\kappa \sim 71 \text{ cm}^2 \text{ g}^{-1} @ 15 \text{ \AA}$

$$\dot{M} = 1.6 \times 10^{-6} M_{\text{sun}}/\text{yr}$$

...so, a **factor of ~4** reduction in mass-loss rate over literature value(s) of $\sim 6 - 8 \times 10^{-6}$

Porosity reduces effective opacity of wind



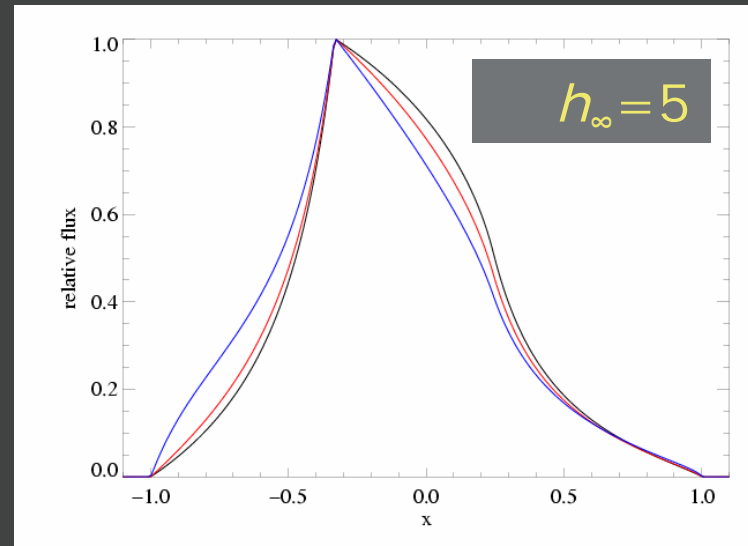
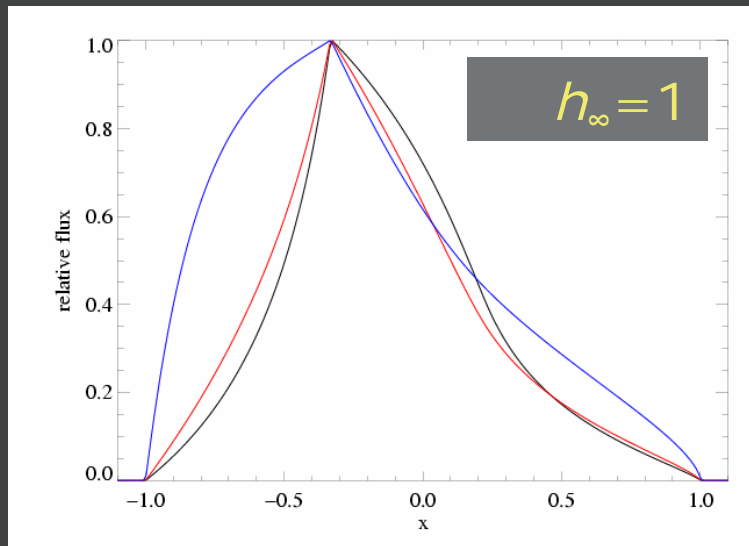
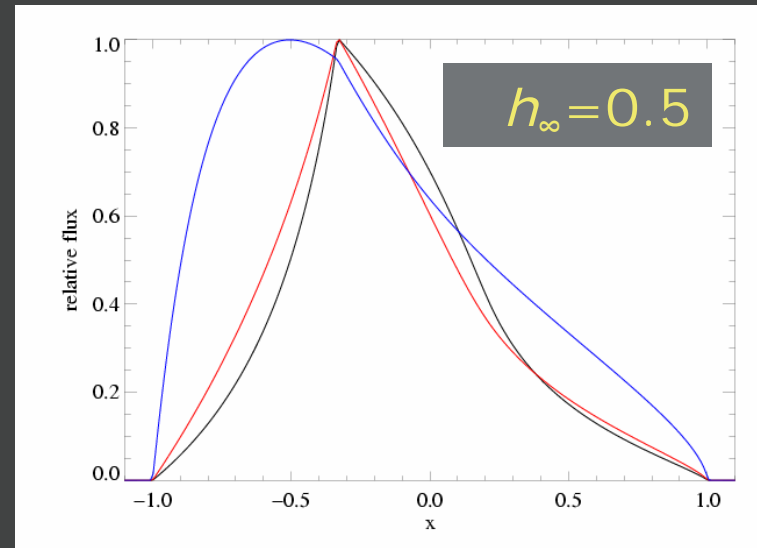
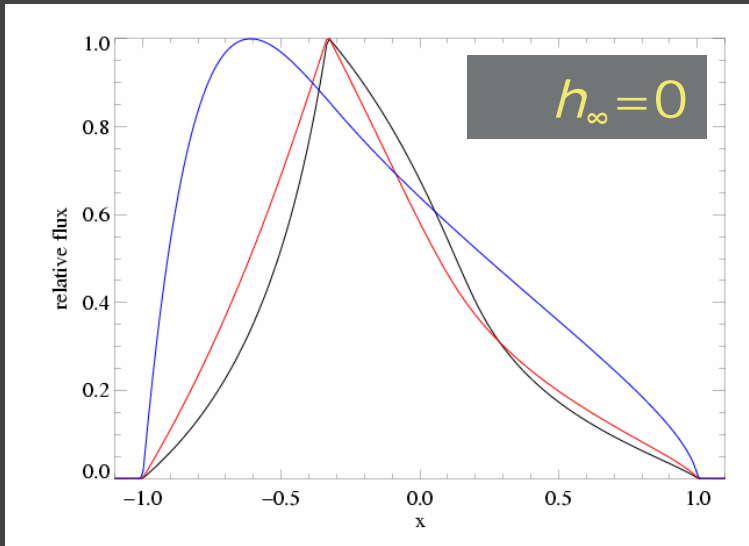
by R. Townsend

The key parameter is the **porosity length**,
$$h = (L^3/l^2) = l/f$$

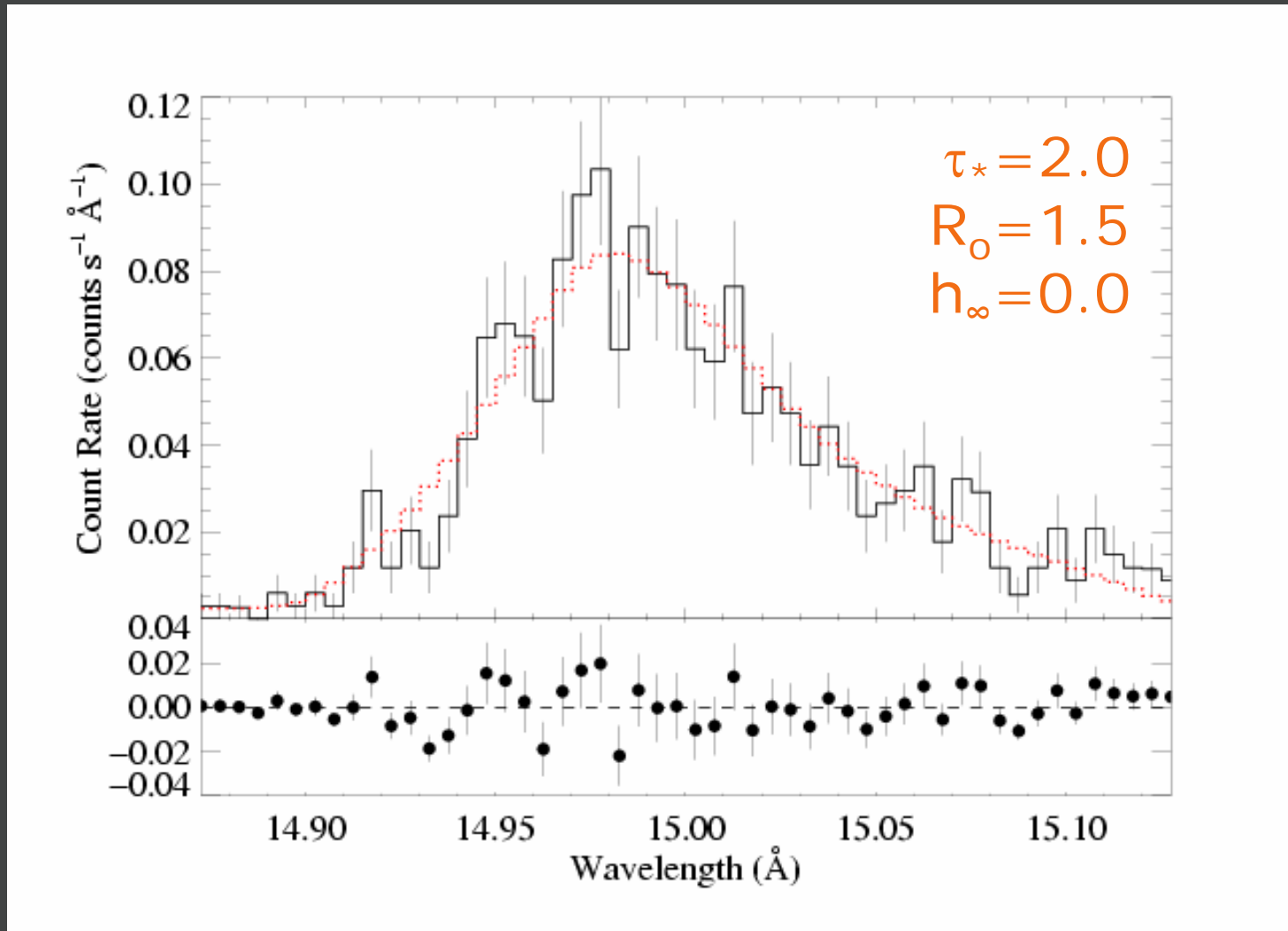
Porosity reduces the effective wind optical depth once h becomes comparable to r/R_*

Optical depth integral modified according to the clumping-induced effective opacity:

$$\kappa_{eff} = \frac{\kappa(1 - e^{-\tau_c})}{\tau_c}$$

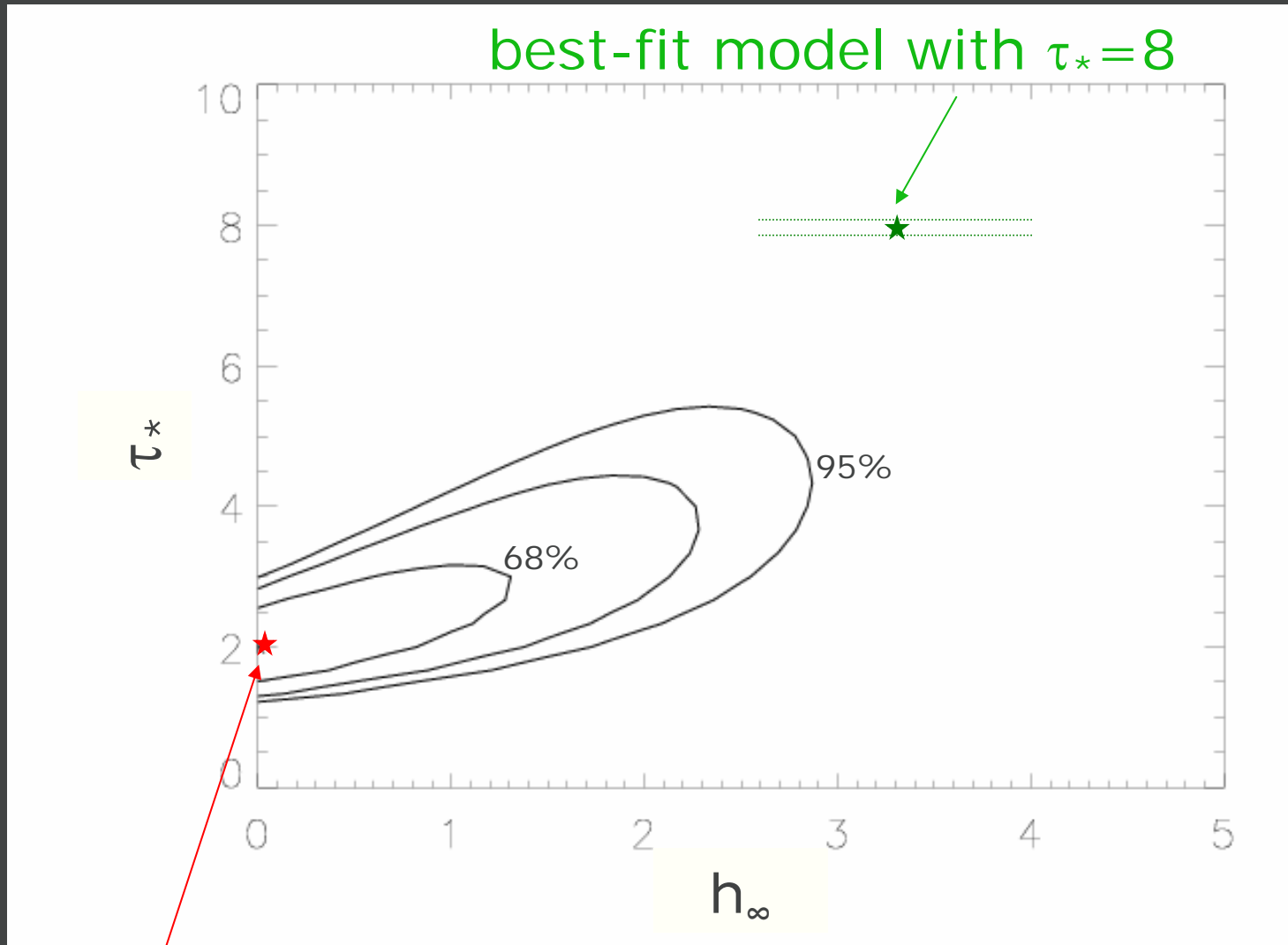


Fitting models that include porosity from spherical clumps
in a beta-law distribution: $h=h_{\infty}(1-R_*/r)$



*Identical to the smooth wind fit: $h_{\infty} = 0$ is
the preferred value of h_{∞} .*

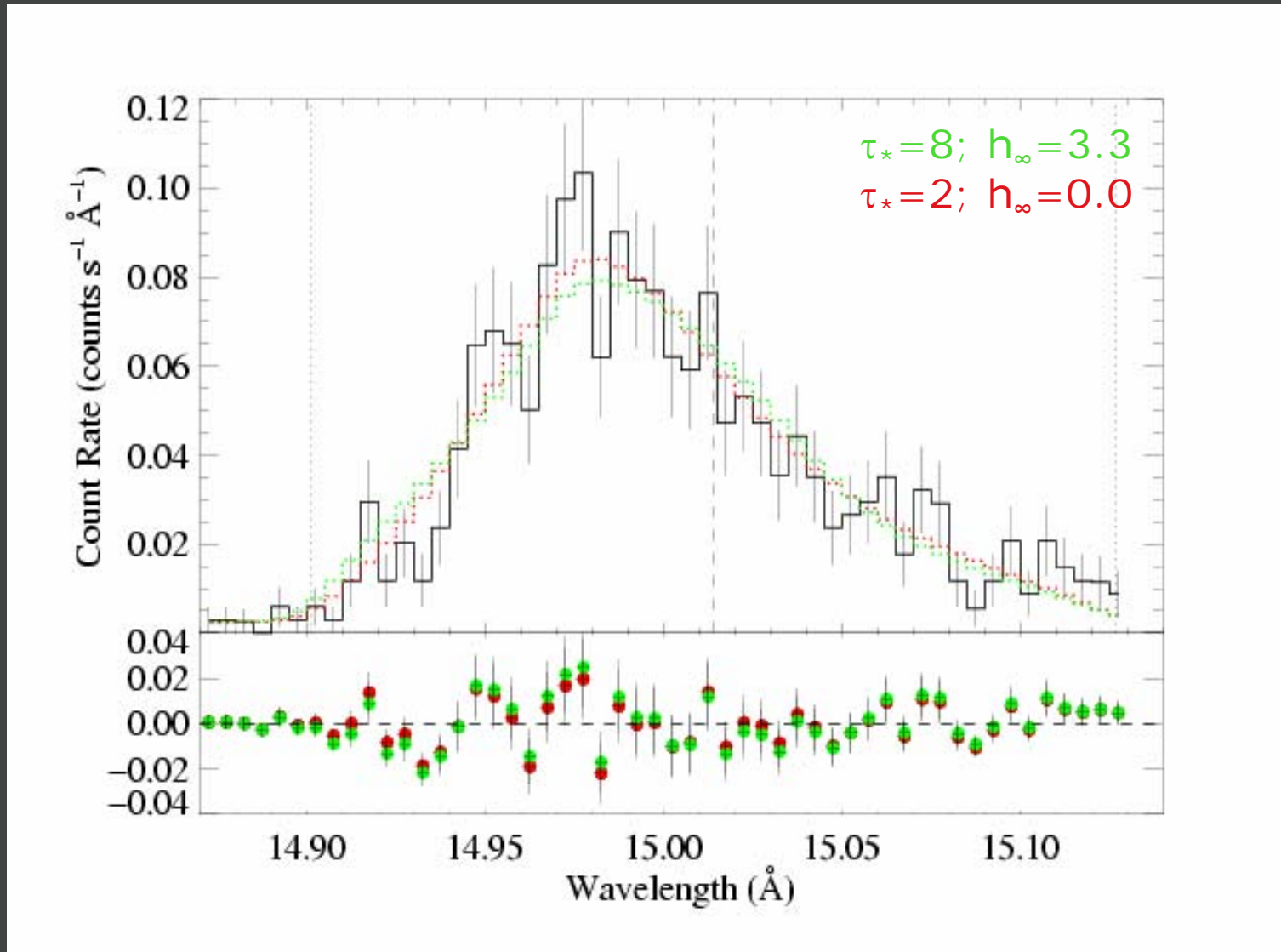
Joint constraints on τ_* and h_∞



best-fit model

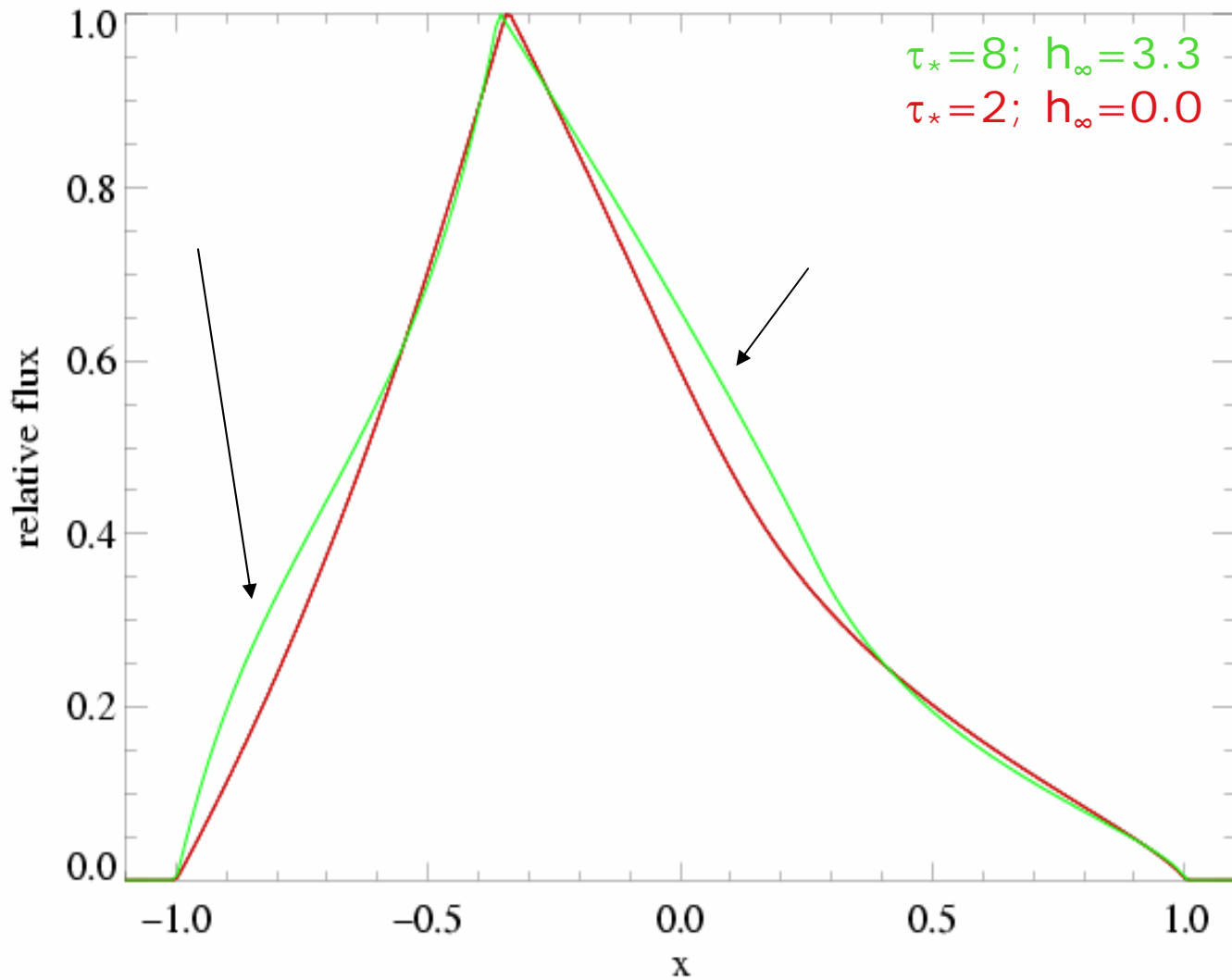
$\Delta C = 9.4$: best-fit model is preferred over $\tau_* = 8$ model with $> 99\%$ confidence

The differences between the models are subtle...

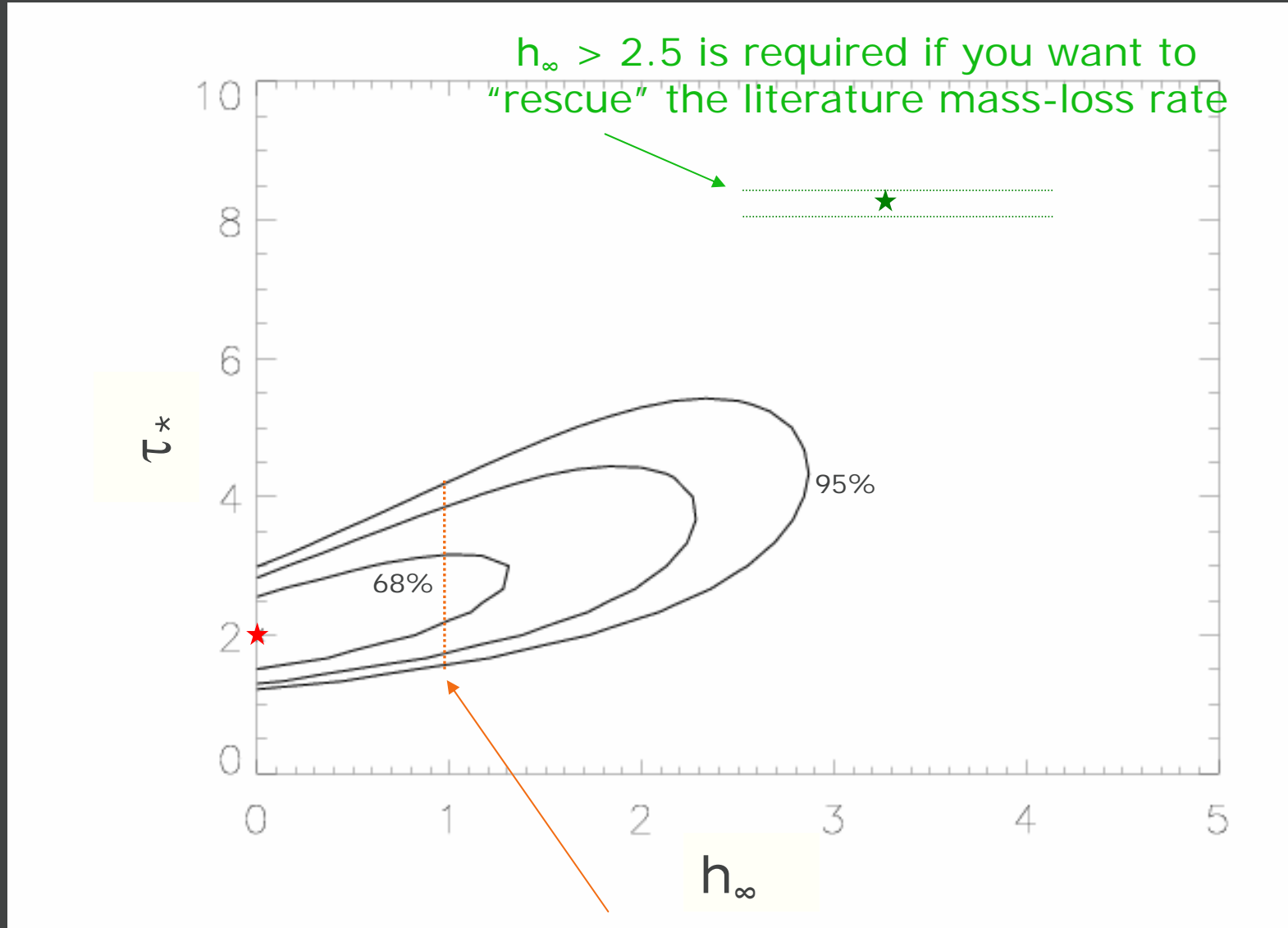


...but statistically significant

Two models from previous slide,
but with *perfect resolution*

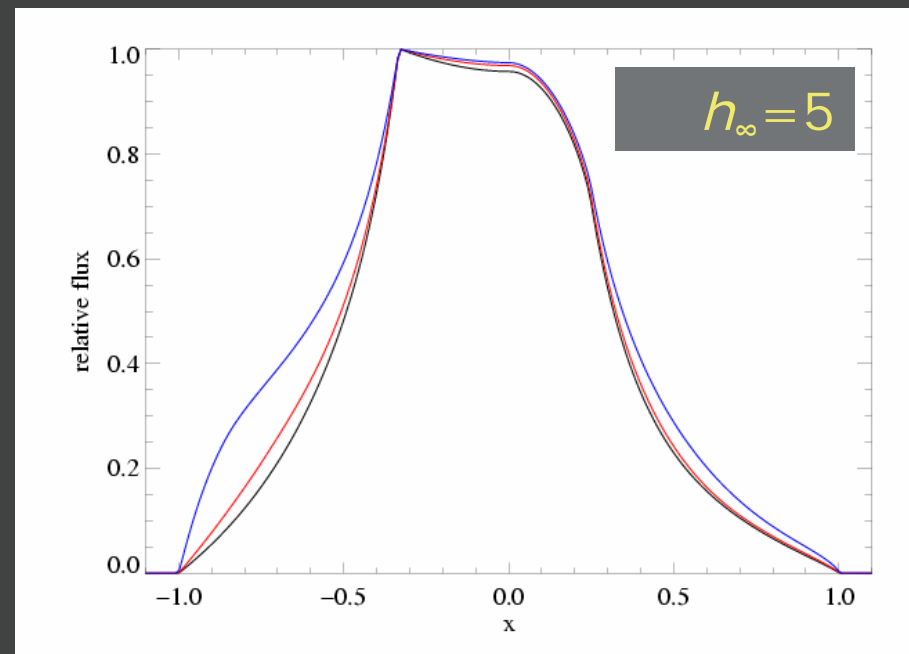
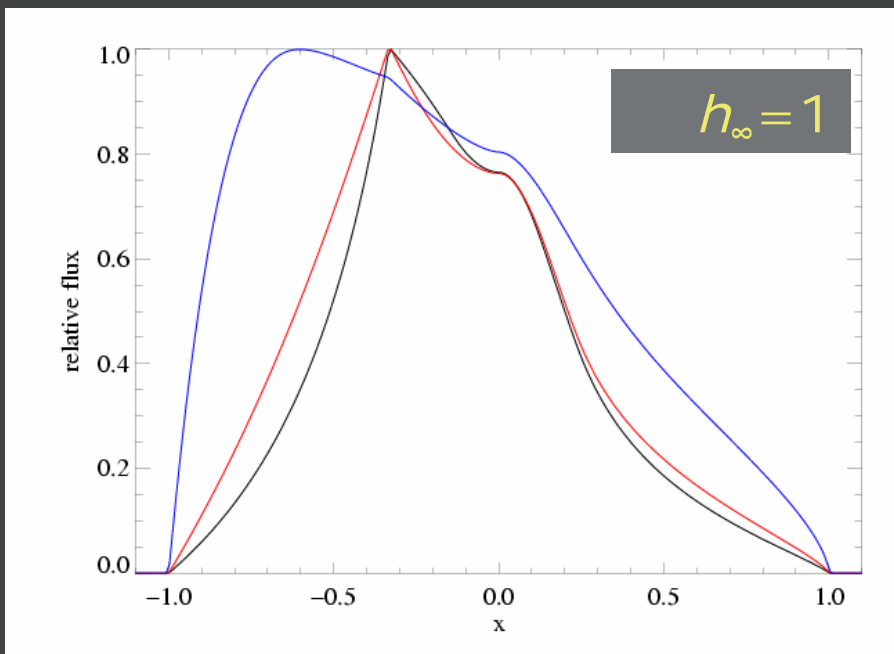
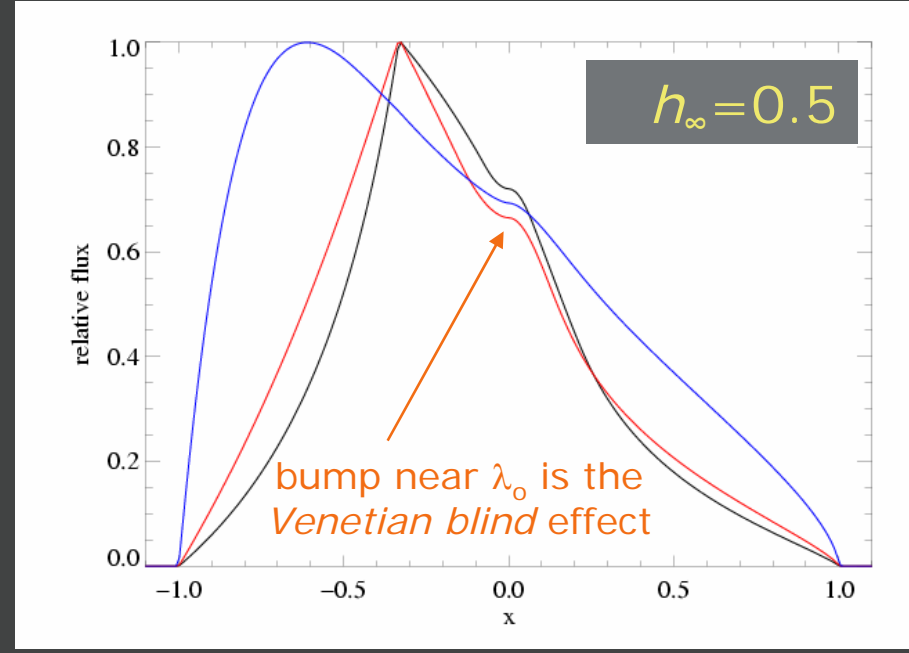
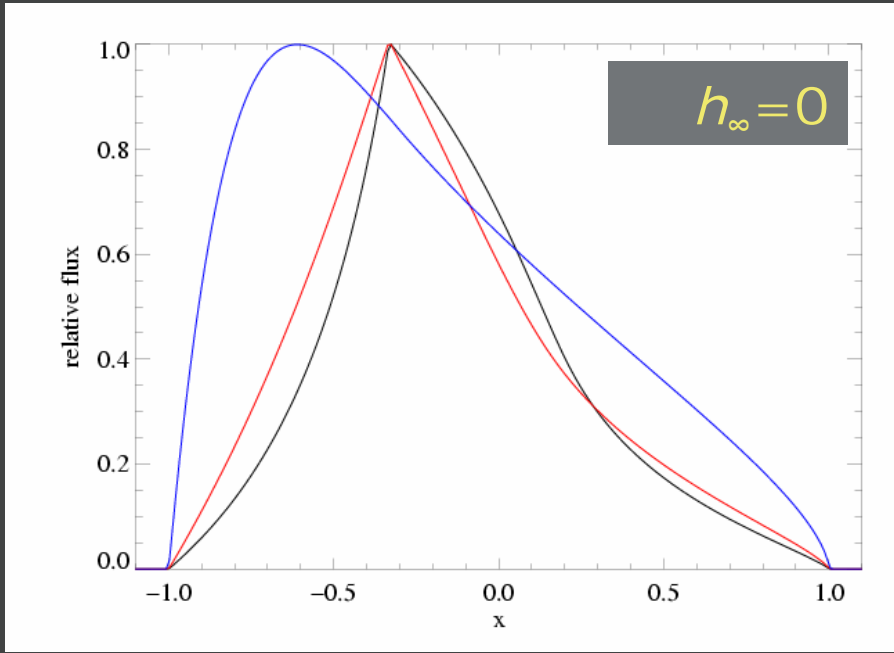


Joint constraints on τ_* and h_∞

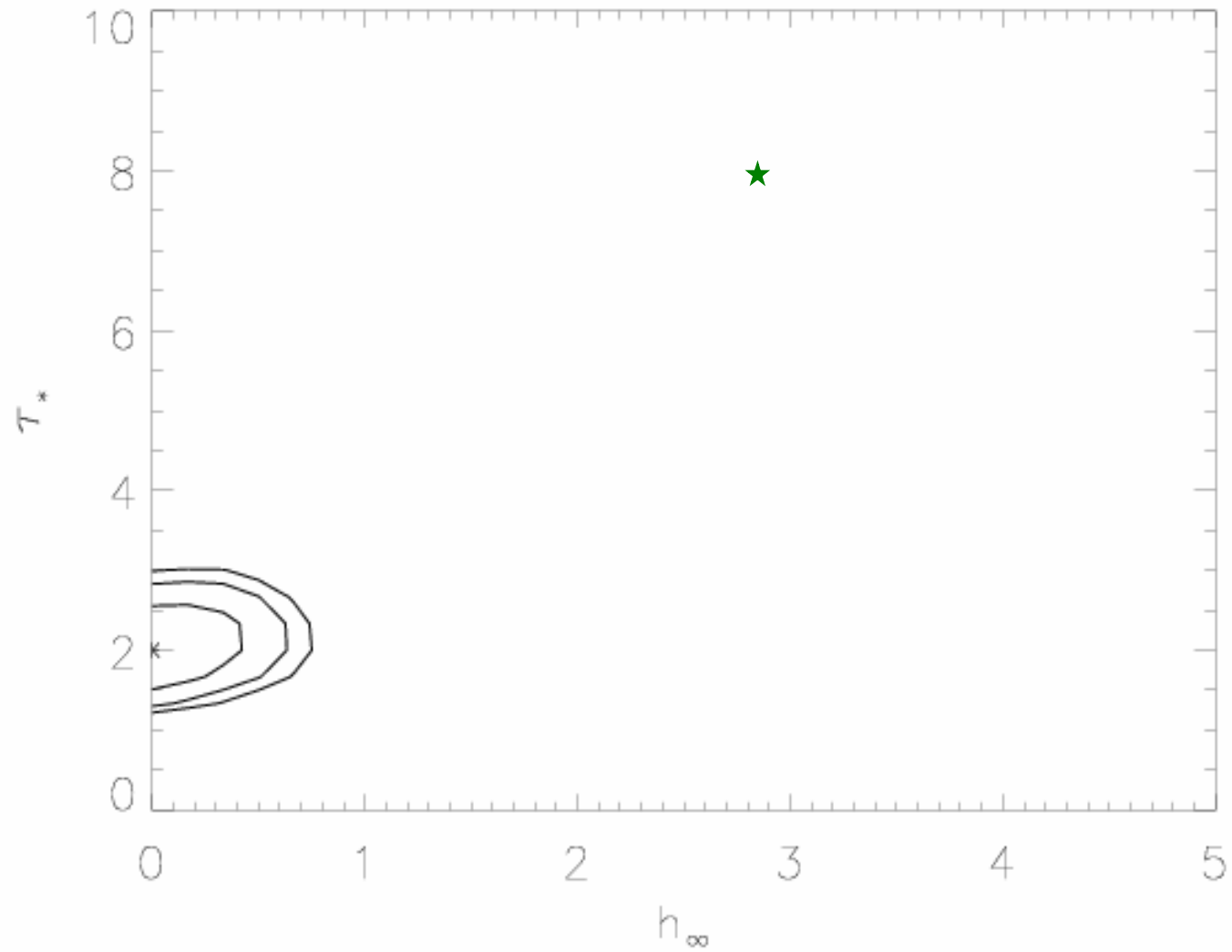


Even a model with $h_\infty = 1$ only allows for a slightly larger τ_*

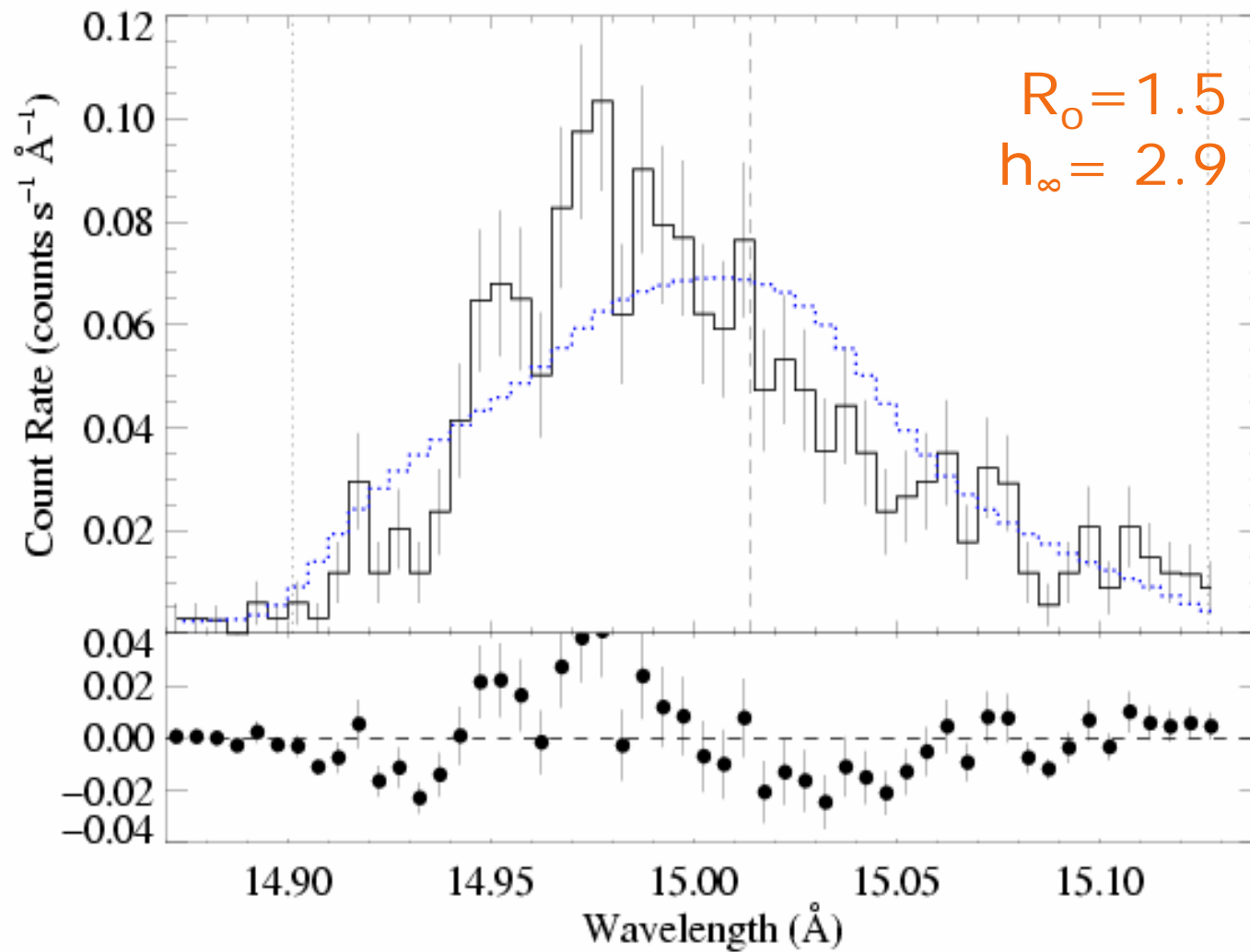
Anisotropic porosity (pancakes): $\tau_{\text{aniso}} = \tau_{\text{iso}}/\mu = \kappa\rho h/\mu$



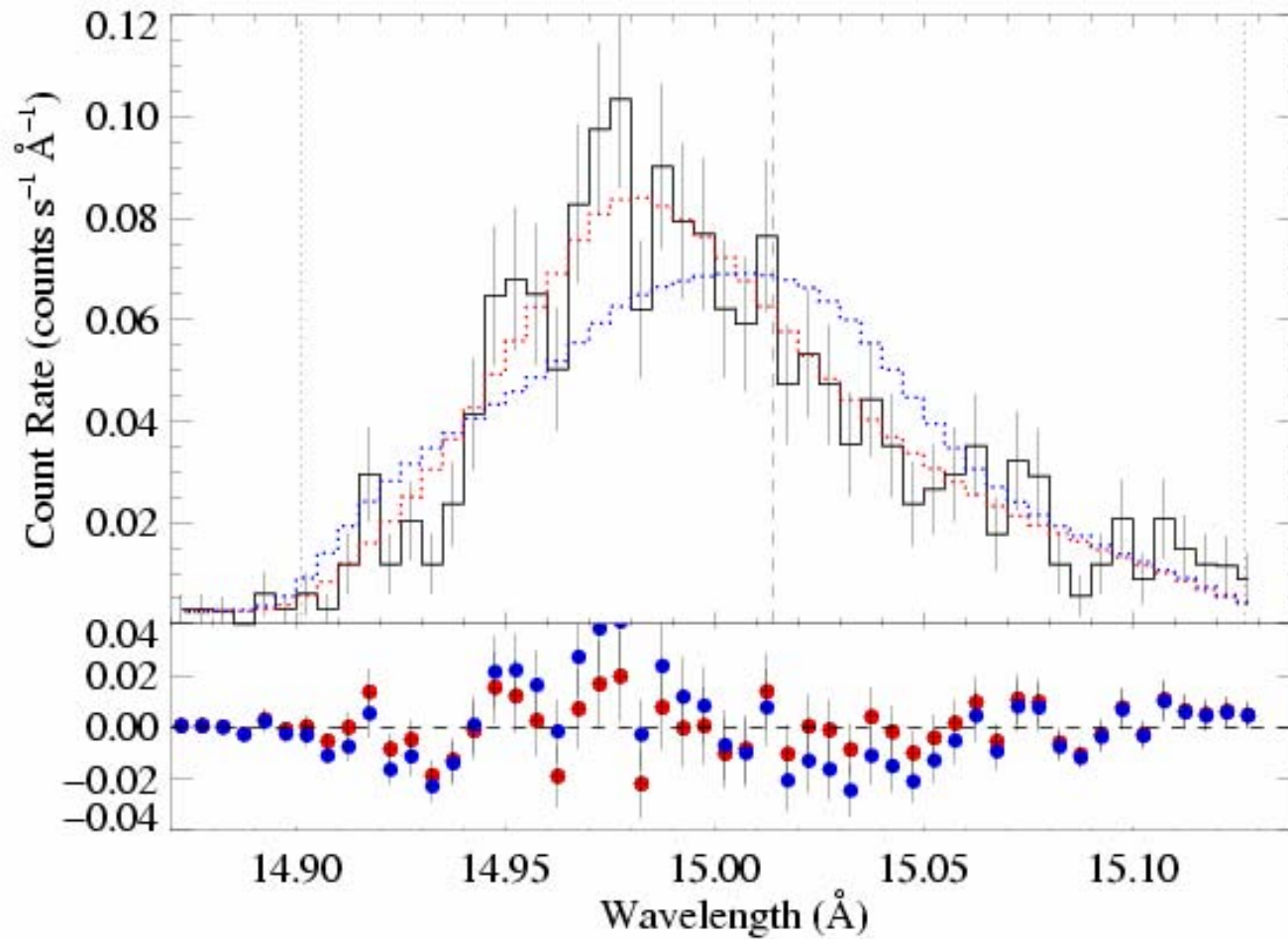
Best-fit model has $h_\infty = 0$



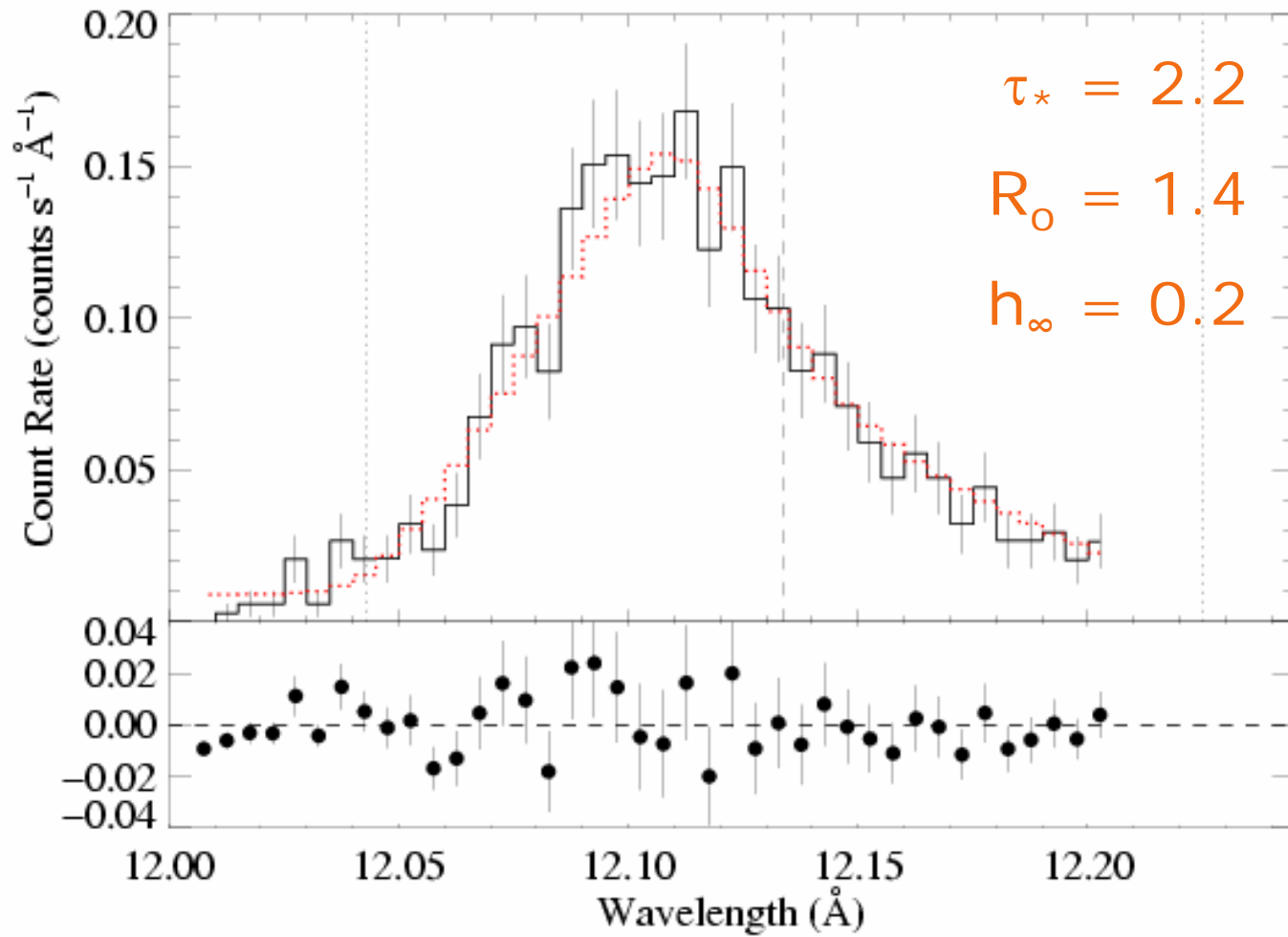
Best-fit *anisotropic* porosity model with $\tau_* = 8$

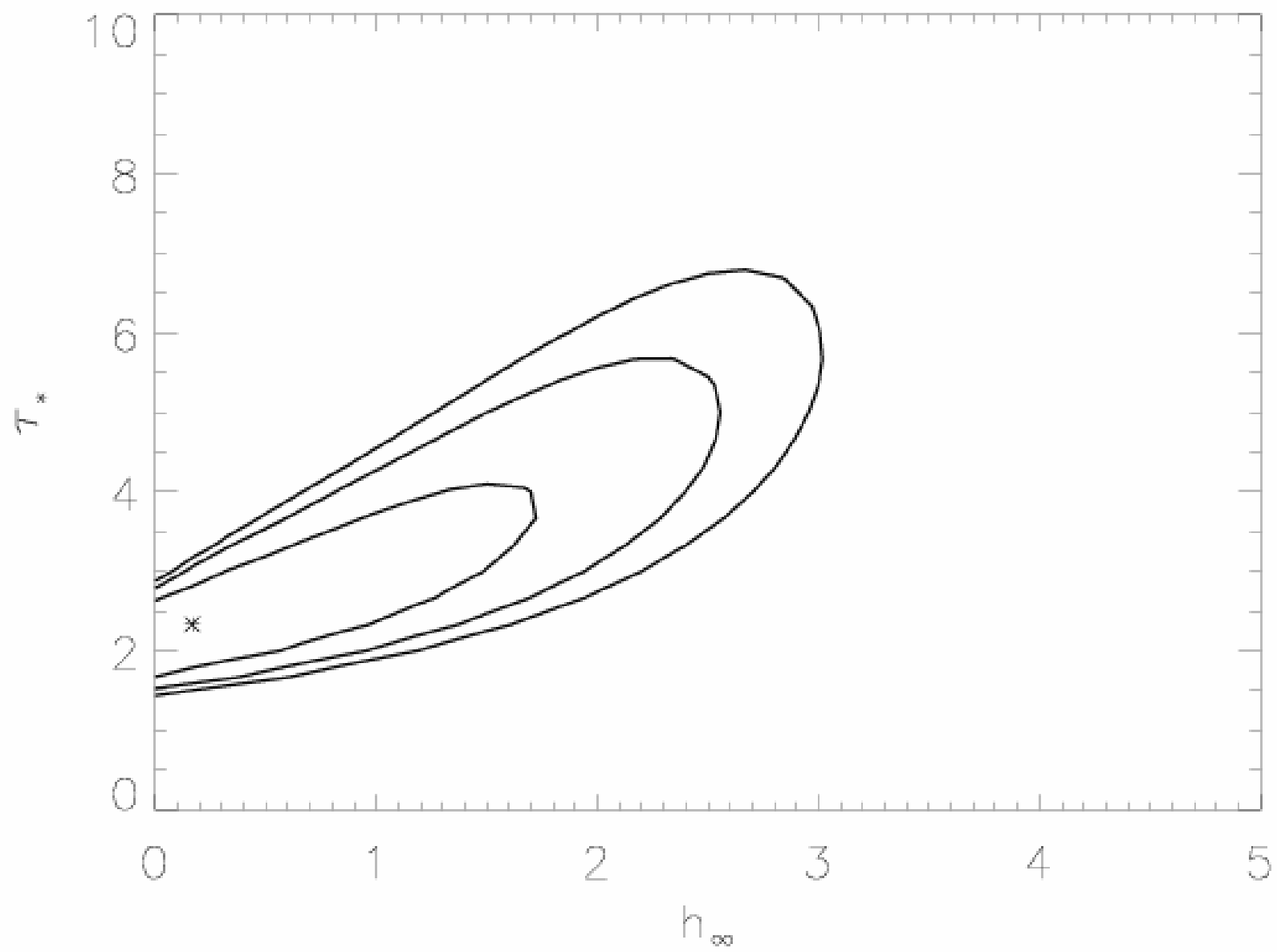


$\Delta C = 31$, aniso-porous model rejected at $P > 99.99\%$



ζ Pup: Ne X Ly- α @ 12.13 Å

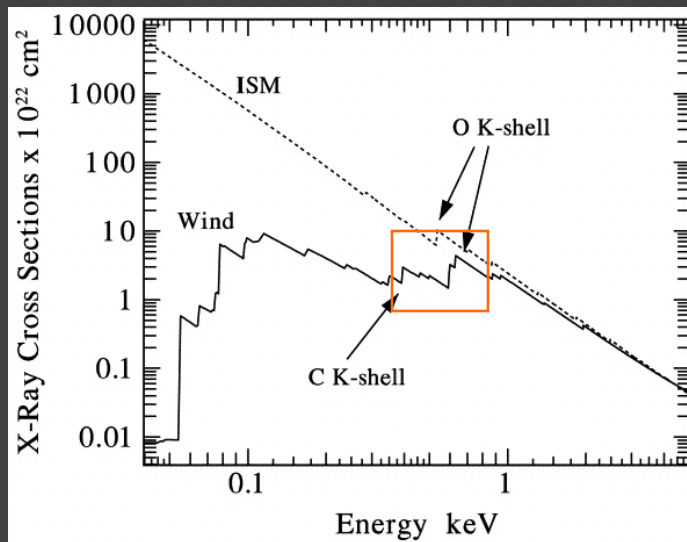




effective opacity: gray?

This is explained naturally by a porosity-dominated wind;

But, atomic opacity is also quite gray over the relevant wavelength range.



Waldron et al. 1998, *ApJS*, 118, 217

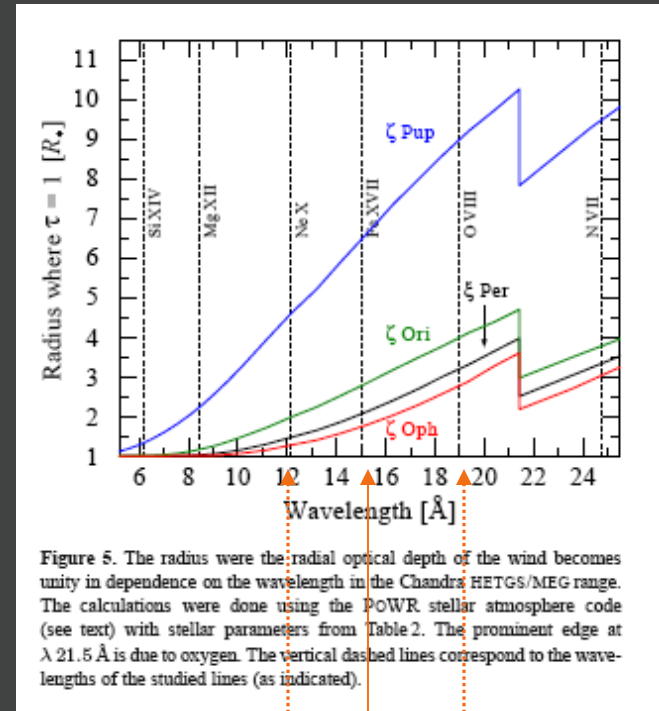
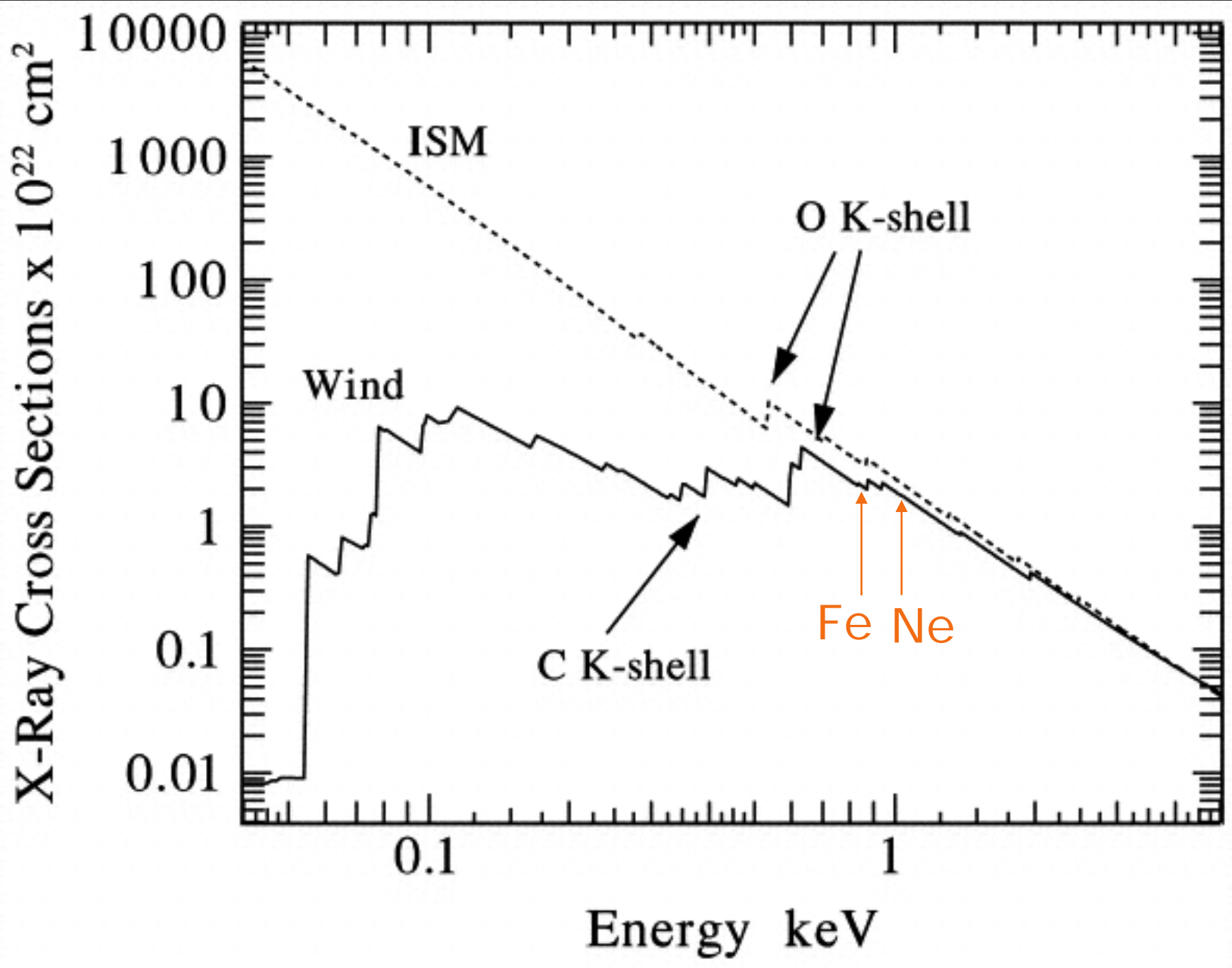


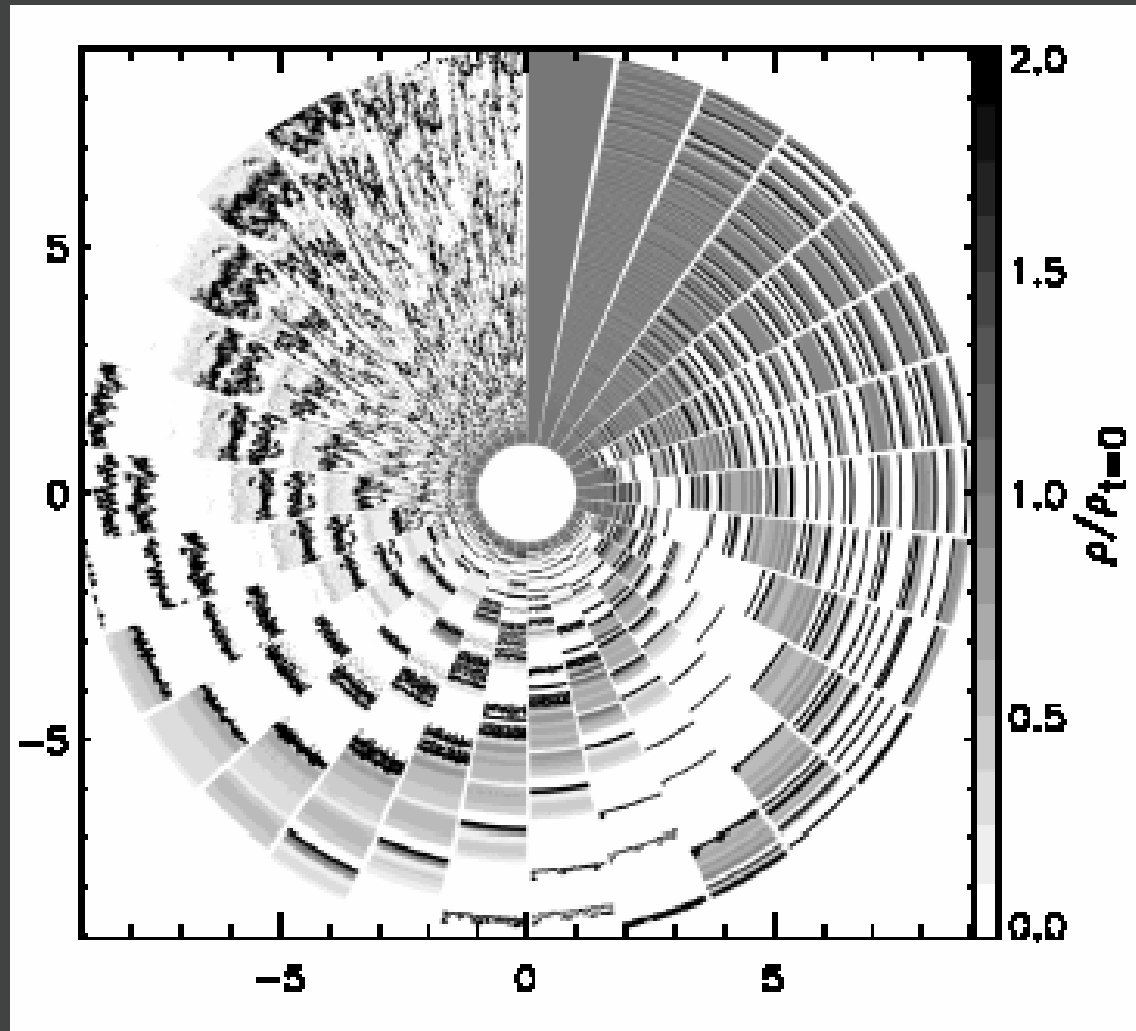
Figure 5. The radius where the radial optical depth of the wind becomes unity in dependence on the wavelength in the Chandra HETGS/MEG range. The calculations were done using the POWER stellar atmosphere code (see text) with stellar parameters from Table 2. The prominent edge at λ 21.5 Å is due to oxygen. The vertical dashed lines correspond to the wavelengths of the studied lines (as indicated).

OFH2006

Fe XVII @ 15 Å

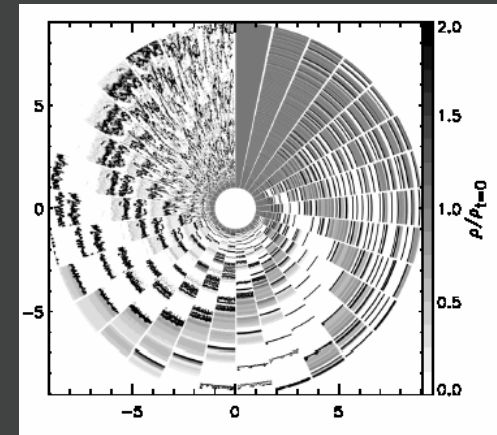


Large porosity lengths are *not* expected from the line-driven instability

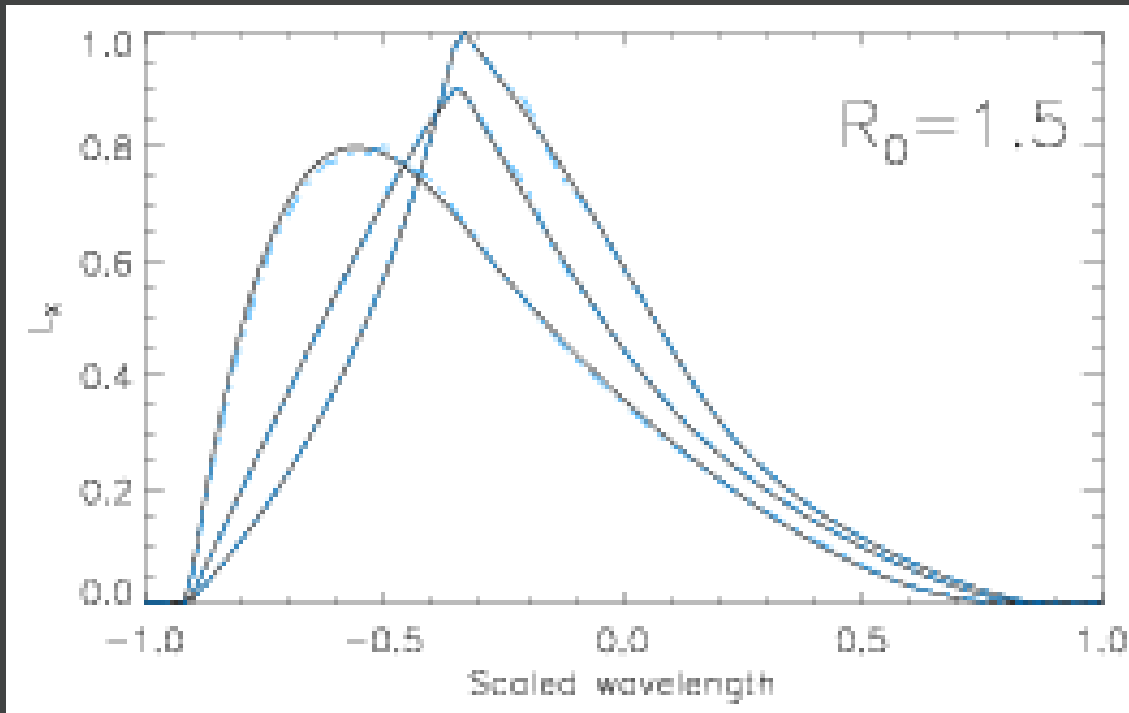


Dessart & Owocki 2003, *A&A*, 406, L1

Profiles synthesized from the 2-D simulations on the previous slide (blue dashed) compared to those from a smooth wind (black solid).



The clumping structure from state-of-the-art simulations has **no effect** on the line profiles.



profiles calculated
assuming $\tau_* = 1, 2, 5$

Courtesy: Luc Dessart

CONCLUSIONS

Smooth-wind emission and absorption models provide good fits to the data.

Mass-loss rate reductions of a factor of 3 to 5 are required.

Models with isotropic porosity provide poorer fits, but cannot yet be definitively ruled out.

CONCLUSIONS, pt. II

However, for porosity to eliminate the need for mass-loss rate reduction, porosity lengths >2.5 are required.

2-D numerical simulations of wind structure generate much smaller porosity lengths.

Anisotropic porosity (pancakes) provides even worse fits to the data than models with isotropic porosity (spheres).

The relative grayness of the effective opacity over the range that includes the strong lines in the *Chandra MEG* can be understood in terms of realistic, detailed wind opacity models.